

Ultrafast single-shot 3D photoacoustic tomography *in vivo* using a single-element detector

Yide Zhang^{1†}, Peng Hu^{1†}, Lei Li¹, Rui Cao¹, Anjul Khadria¹, Konstantin Maslov¹, Xin Tong¹, Yushun Zeng^{2,3}, Laiming Jiang^{2,3}, Qifa Zhou^{2,3}, and Lihong V. Wang^{1*}

¹Caltech Optical Imaging Laboratory, Andrew and Peggy Cherng Department of Medical Engineering, Department of Electrical Engineering, California Institute of Technology, Pasadena, CA 91125, USA

²USC Roski Eye Institute, University of Southern California, Los Angeles, CA 90033, USA

³Alfred E. Mann Department of Biomedical Engineering, University of Southern California, Los Angeles, CA 90089, USA

† These authors contributed equally.

* Correspondence should be addressed to L.V.W. (LVW@caltech.edu)

We introduce photoacoustic computed tomography through an ergodic relay (PACTER), offering ultrafast 3D imaging of hemodynamics. A single-element detector in PACTER encodes information equivalent to that of 6,400 virtual ones, allowing real-time imaging of rapid hemodynamics. The PACTER system is calibrated once before imaging using a procedure where the laser beam is transmitted through the ergodic relay and focused on a uniform optical absorber (Fig. 1a). After calibration, the system is ready for imaging, and the focusing lens is replaced by a fly's eye homogenizer, converting the laser beam into a widefield, and

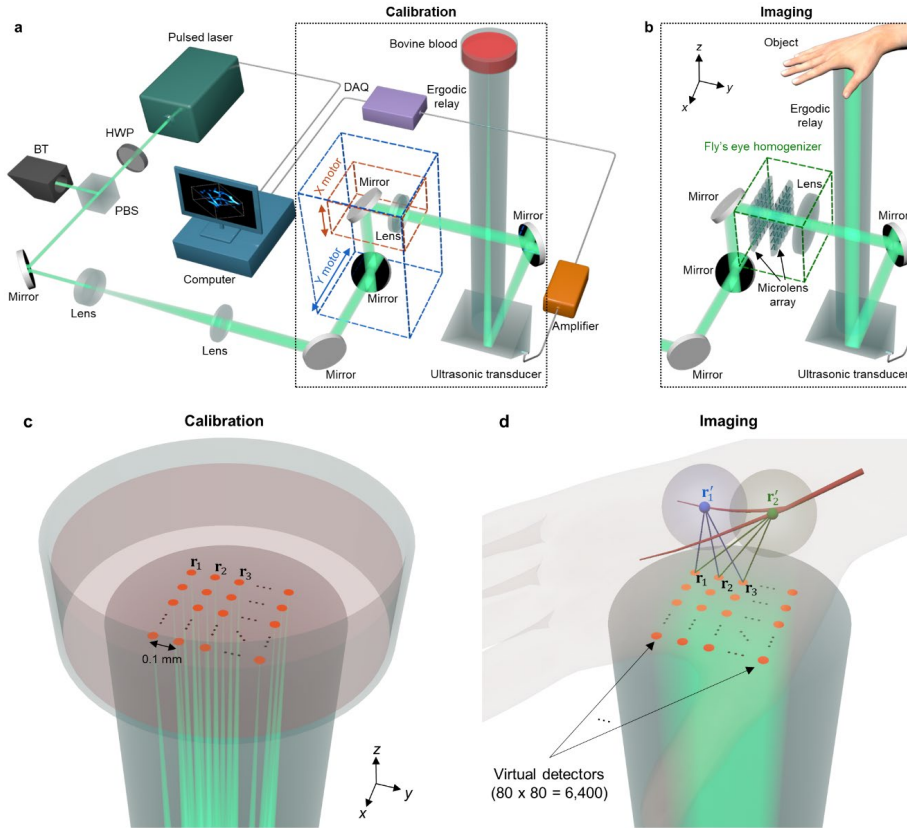


Fig. 1 PACTER principle. **a,b**, Schematic of the PACTER system in the calibration (**a**) and imaging (**b**) procedures. HWP, half-wave plate; PBS, polarizing beam splitter; BT, beam trap; DAQ, data acquisition unit. The differences between the two modes are highlighted in the black dotted boxes. **c**, Illustration of the calibration procedure of PACTER. Focused laser beams for calibration are shown in green. Calibration pixels are highlighted as orange dots. Calibration step size is 0.1 mm. The calibration pixels (80×80) become 6,400 virtual transducers. \mathbf{r}_1 , \mathbf{r}_2 , \mathbf{r}_3 are the positions of three calibrated virtual transducers. **d**, Illustration of PACTER of human palmar vessels. The homogenized beam for widefield illumination is shown in green. \mathbf{r}'_1 and \mathbf{r}'_2 are the positions of two source points in the vessels. Blue and green spheres denote the PA waves generated by the source points. The calibrated virtual transducers capture the PA signals from \mathbf{r}'_1 and \mathbf{r}'_2 with different delays, indicated by the thick blue and green lines.

homogenized illumination pattern (Fig. 1b). During the calibration procedure, the focused laser beam was scanned across the field of view (FOV) in a grid of 80 by 80 steps, each being 0.1 mm (Fig. 1c). Although this scanning was conducted on a 2D plane, the calibration signals were utilized as 6,400 virtual transducers for 3D reconstruction (Fig. 1d).

PACTER shows promise for monitoring live hemodynamics. We first used PACTER to monitor vital signs in small animals, specifically imaging the abdominal regions of mice (Fig. 2a). A single laser pulse allowed PACTER to reconstruct 3D images of abdominal blood vessels (Fig. 2b), while multiple pulses revealed their 4D dynamics (Fig. 2c). The movements and structural alterations of individual blood vessels can be visualized (Fig. 2d).

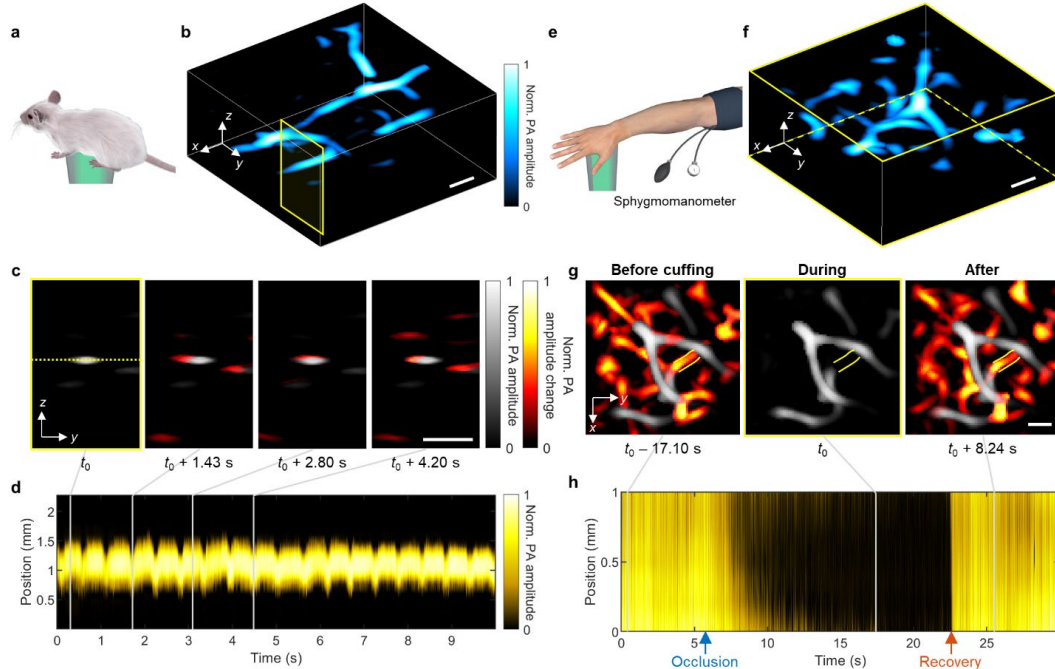


Fig. 2 PACTER results. **a**, Schematic of the mouse imaging experiment. **b**, 3D PACTER image of the abdominal vasculature of the mouse. **c**, Cross-sectional 2D images corresponding to the yellow rectangle in **b** at four different time instances from the 4D PACTER datasets. $t_0 = 0.28$ s. Differences from the first image are highlighted. **d**, PA amplitudes along the yellow dashed line (1D images) in **d** versus time, where the time instances in **c** are labeled with vertical gray lines. **e**, Schematic of the human hand imaging experiment. **f**, 3D PACTER image of the thenar vasculature of the participant. **g**, Maximum amplitude projections of the 3D volumes from the 4D PACTER datasets along the z axis in **f** at the time instances before, during, and after cuffing. $t_0 = 17.44$ s. The solid lines flank the vessels under investigation. Differences from the images during cuffing are highlighted. **h**, PA amplitudes along the vessels (1D images) in **g** versus time, where the time instances in **g** are labeled with vertical gray lines. The blue and orange arrows indicate peak responses in the occlusion and recovery phases, respectively. Norm., normalized. Scale bars, 1 mm.

To show the effectiveness of PACTER in human hemodynamics monitoring, we then used PACTER to monitor the thenar vasculature of a human participant and its response to cuffing, induced by a sphygmomanometer (Fig. 2e). Using PACTER, 3D images of the thenar vasculature were taken with single laser pulses (Fig. 2f), and the 4D dynamics of blood vessels were reconstructed during cuffing (Fig. 2g). The data revealed that while some blood vessels maintained constant PA amplitude throughout the experiment, others showed a decrease due to blood flow occlusion. When the cuffing was released, the blood flow and PA amplitude were quickly restored (Fig. 2h).

The study demonstrates PACTER's effectiveness in non-invasively monitoring hemodynamics, providing insights into blood vessel dynamics both in animals and humans, and showing its potential for detailed observation of blood flow and amplitude responses, making it a valuable tool for future medical applications.